JMEPEG (2005) 14:367-372
DOI: 10.1361/10599490524020

1059-9495/$19.00

Effects of Low-Temperature Aging on AISI 444 Steel

José A. Souza, Hamilton F.G. Abreu, Alex M. Nascimento, José A.C. de Paiva, Pedro de Lima-Neto, and Sérgio S.M. Tavares

(Submitted October 4, 2004; in revised form December 31, 2004)

The consequences of aging at 400 and 475 °C on the mechanical properties, corrosion resistance, and magnetic properties of the ferritic stainless steel (SS) AISI 444 were investigated. Age hardening was measured as a function of aging time at both temperatures and was found to be more intense at 475 °C. The localized corrosion susceptibility increased, while the impact toughness decreased with aging time. These two effects were also more important at 475 °C. Unlike duplex SSs, AISI 444 did not present any variation in coercive force or Curie temperature with aging time. The effects on the Mössbauer spectra were also determined and analyzed.

Keywords: AISI 444 steel, corrosion resistance, embrittlement, ferritic stainless steels

1. Introduction

Ferritic stainless steels (SSs) are used in many manufacturing processes, mainly in the petrochemical industries. The main advantage of ferritic steels over the austenitic grades (e.g., 304 SS or 316 SS) is superior stress corrosion resistance. However, ferritic SSs are susceptible to some embrittlement phenomena such as grain growth, σ-phase formation (Ref 1, 2), and α′-precipitation (Ref 2, 3).

The precipitation of α′ occurs at between 350 and 550 °C in ferritic and duplex SSs (Ref 2-4). According to Grobner (Ref 3), α′ formation in ferritic SSs with <17% Cr occurs by nucleation and growth, while above this level it occurs by spinodal decomposition, as in, for example, duplex SSs.

The susceptibility of the ferritic steels to the α′ precipitation increases with Cr, Mo, and Si contents. The main reported effects of α′ in ferritic and duplex steels are decreases of toughness, increases of hardness, and corrosion-resistance decay. A change in the magnetic properties is also observed (Ref 5-9), and, therefore, can be used to detect the embrittlement stage in ferritic and duplex steels (Ref 7-9). Ferritic SSs are also susceptible to sensitization due to the precipitation of carbides while in the 425 to 700 °C temperature range (Ref 10).

In the present work, the effects of low-temperature aging of AISI 444 SS were investigated. This study is motivated by the possible substitution of AISI 316L SS by AISI 444 SS in the distillation towers of petroleum-refining plants. AISI 444 SS is cheaper than the 316 grade and exhibits similar corrosion resistance due to Mo additions.

José A. Souza, Hamilton F.G. Abreu, and **Alex M. Nascimento,** Universidade Federal do Ceará, Departamento de Engenharia Mecânica/Laboratório De Caracterização De Materiais, Campus do Pici, Bloco 714, 60455-760, Fortaleza-CE, Brazil; **José A.C. de Paiva,** Universidade Federal do Ceará, Departamento de Física, Fortaleza, Brazil; **Pedro de Lima-Neto,** Universidade Federal do Ceará, Departamento de Química Analítica e Físico-Química, Fortaleza, Brazil; and **Sérgio S.M. Tavares,** Universidade Federal Fluminense, Departamento de Engenharia Mecânica/Pós-Graduação em Engenharia Mecânica, Niterói, Brazil. Contact e-mail: ssmtavares@ig.com.br.

2. Experimental

The chemical composition of AISI 444 is shown in Table 1. The mean hardness of the as-received steel was 187 ± 1 HV. The samples were heat-treated at 400 and 475 °C for times between 10 and 1000 h. These temperatures were selected because 400 °C is the maximum operational temperature in the distillation tower, while 475 °C is reported to be the temperature at which the kinetics of α′ precipitation reach a maximum (Ref 3). Regeneration treatments at 570 and 675 °C were used on samples that were aged at 475 °C for 1000 h. Vickers hardness measurements used a load of 30 kg in all conditions.

AISI 444 steel is very notch-sensitive. Using Charpy V-notch reduced size samples (2.5 mm), a very small energy

Table 1 Chemical composition of AISI 444 (in weight percent)

C	Cr	Ni	Mo	Ti	Si	N	Fe
0.015	17.56	0.20	1.86	0.13	0.54	0.0123	Balance

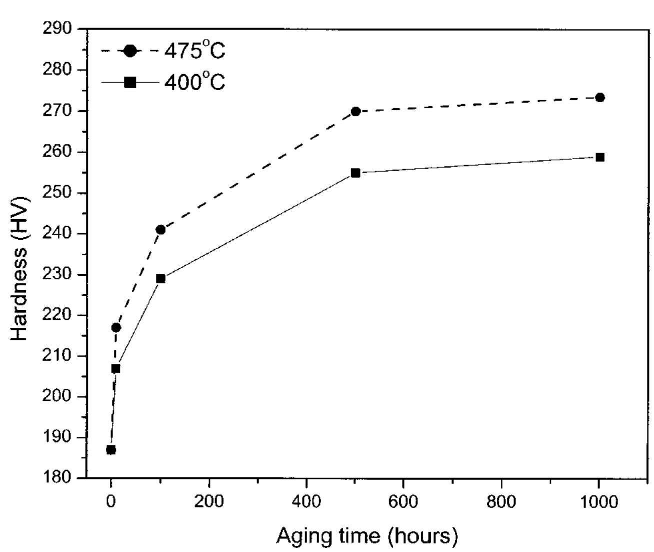

Fig. 1 Hardness against aging time at 400 and 475 °C

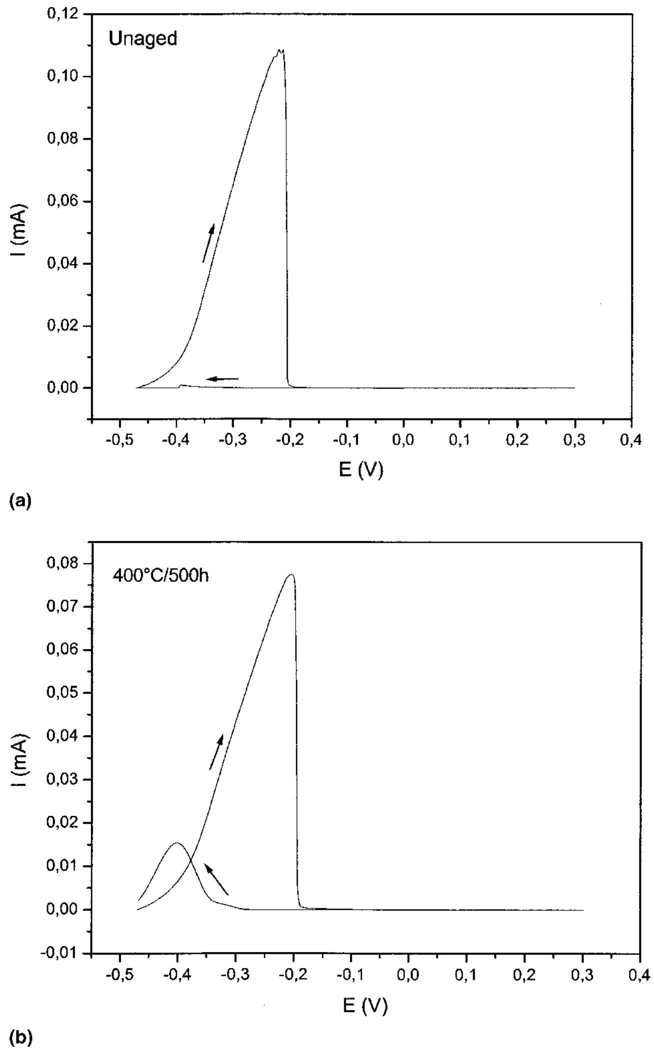

Fig. 2 The DL-EPR curves obtained in the (a) as-received sample and (b) in the sample aged at 400 °C for 500 h

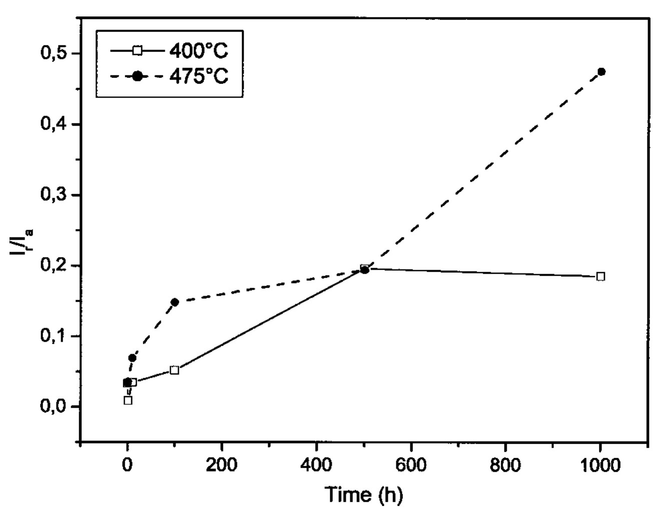

Fig. 3 Th ratio of I_r to I_a against aging time at 400 and 475 °C

value for fracture (3 J) was measured in the as-received condition. On the other hand, using an unnotched sample, the fracture energy increased to 120 J. For this reason, unnotched

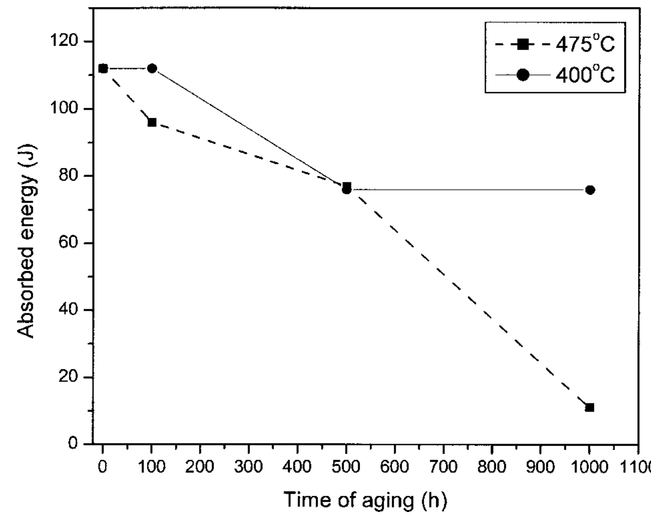

Fig. 4 Absorbed energy to fracture against aging time at 400 and 475 °C

specimens were used to evaluate the effects of aging on toughness. Two samples at each aging condition were machined to 55 × 10 × 2.5 mm, and then were tested using a universal impact test machine with a maximum capacity of 300 J and a precision of ± 1 J.

The corrosion resistance was evaluated using double-loop electrochemical potentiodynamic reactivation (DL-EPR) tests. This is a practical and simple test, which was developed to detect and quantify sensitization in austenitic SSs (Ref 10). Some authors have used this test to study the corrosion resistance of duplex SSs aged at high (Ref 11) and low (Ref 12) temperatures. In this work, the DL-EPR tests were conducted using a conventional three-electrode cell with Pt foil as the auxiliary electrode and a saturated calomel electrode (SCE) as the reference electrode. The working electrode was constructed using AISI 444 steel samples embedded in epoxy resin. The experiments were initiated after a nearly steady-state open-circuit potential (E_{oc}) had been achieved (after ~30 min), followed by the potential sweep in the anodic direction at 1 mV/s until a potential of 0.3 V (versus SCE) was reached. Then, the scan was reversed in the cathodic direction until the E_{oc} was reached. Prior to each experiment, the working electrodes were polished on 400-grit abrasive emery paper. The samples were then degreased with alcohol and cleaned in distilled water. The working solution was 0.5 M H_2SO_4 + 0.01 M KSCN (potassium thiocyanate). The localized corrosion susceptibility was evaluated from the ratio of I_r to I_a, where I_a is the peak current of the anodic scan and I_r is the peak current in the reverse direction (Ref 10). For the best results, the test temperature was 60 °C.

Metallographic samples were etched with a hot 10% HNO_3 + 0.05% HF solution and were observed under an optical microscope.

Magnetic measurements were carried out in a vibrating sample magnetometer with a maximum applied field of 5.0 kOe. Curie temperatures (T_c) were measured using a thermomagnetic balance. Mössbauer spectroscopy measurements made in the transmission mode were made on 0.06 to 0.08 mm thick specimens using a ^{57}Co source on Rh. Machine-specific software was used to fit the measured spectra.

3. Results

3.1 Mechanical Properties and Corrosion-Resistance Degradation

Figure 1 shows the influence of aging time on hardness for AISI 444 SS. The maximum men values were 259.0 ± 3.7 HV and 273.5 ± 6.2 HV at 400 and 475 °C, respectively. The curves are similar in shape, but, as expected, aging at 475 °C yields higher hardness values than at 400 °C. Overaging was not observed. These results are in close agreement with those presented in the literature for Fe-Cr (Ref 3) and Fe-Cr-Ni (Ref 8, 9) alloys, which also showed that the aging yielded more intense changes at 475 °C.

Figure 2 shows the DL-EPR curves obtained for the as-received sample (Fig. 2a) and for one aged at 400 °C for 500 h (Fig. 2b). Both tests were performed at 60 °C. It is worth noting that aged samples tested at 25 °C did not show a reactivation peak, and, therefore, the ratio of I_r to I_a was always zero.

Figure 3 shows the behavior of the ratio of I_r to I_a with aging time. Aging at 475 °C promotes an increase in the ratio of I_r to I_a in the first 10 h of aging. An important increase in the ratio of I_r to I_a was observed from 500 to 1000 h. At 400 °C, the increase in the ratio of I_r to I_a is more gradual, reaching the maximum value (0.20) in the samples aged for 500 and 1000 h.

Figure 4 shows the decrease of toughness with aging time. It is interesting to note the similarity to the corrosion-resistance behavior (Fig. 3). Aging at 400 °C promotes a decrease in toughness until 500 h, where the same value (76 J) is subsequently maintained for additional aging times. The samples aged at 475 °C show a continuous decrease in toughness, with a pronounced decrease in toughness from 500 to 1000 h.

Figure 5 shows surface images of the samples used in the DL-EPR tests. The aged samples are completely attacked (Fig. 5a) while the surface of the unaged sample remains relatively smooth (Fig. 5b). Figures 6 to 8 show the etched microstructures that were revealed using the hot 10% HNO_3 + 0.05% HF solution. The sample aged at 475 °C for 1000 h (Fig. 8a) shows more intense corrosion pitting than the samples aged at 400 °C for 1000 h (Fig. 6a) and at 475 °C for 500 h (Fig. 7). Intergranular attack is also much more intense in the sample aged at 475 °C for 1000 h (Fig. 8b) than that aged for 500 h (Fig. 7). This suggests that the increase of the ratio of I_r to I_a, and the decrease of toughness between 500 and 1000 h at 475 °C, are caused by additional intergranular precipitation.

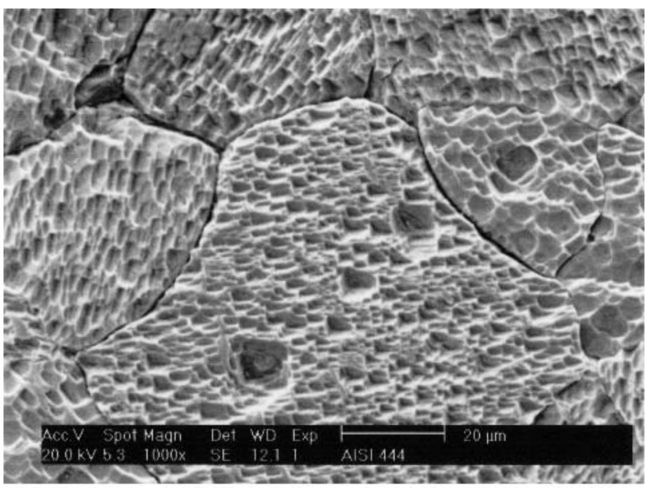

(a)

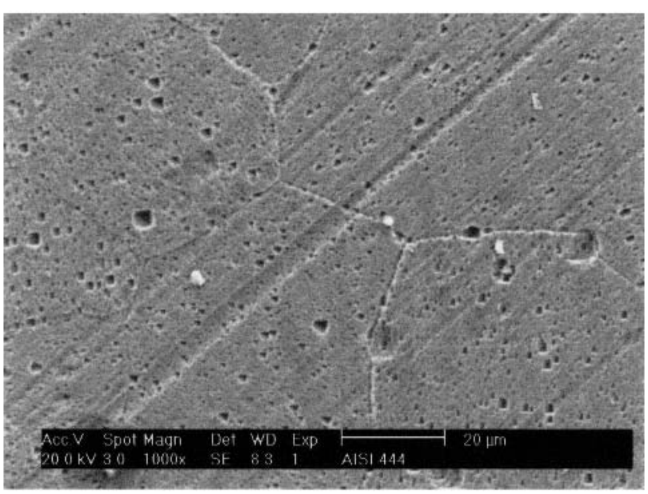

(b)

Fig. 5 Surface image of the samples used in the DL-EPR tests: (a) sample aged at 475 °C for 1000 h; and (b) the unaged sample

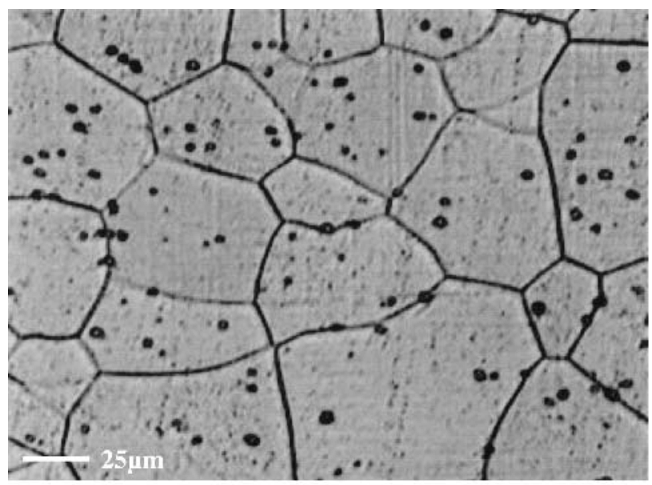

(a)

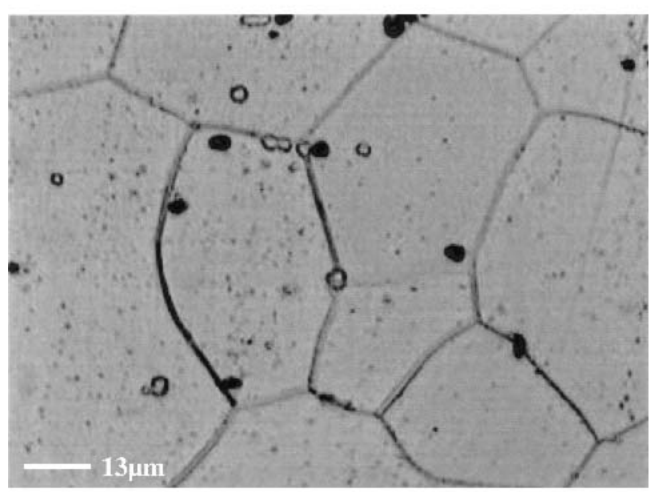

(b)

Fig. 6 Sample aged at 400 °C for 1000 h

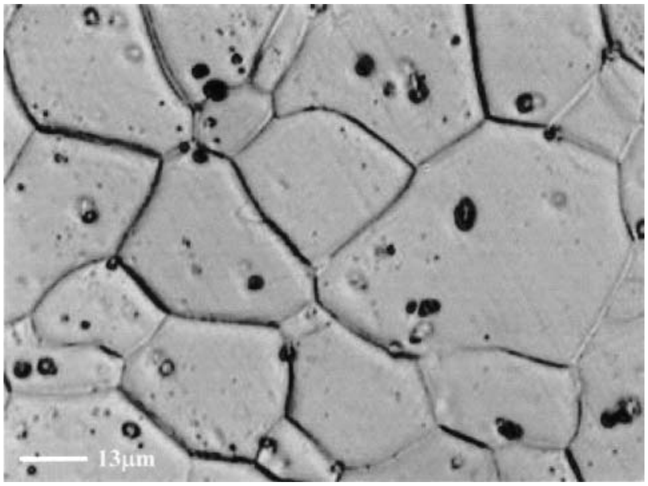

Fig. 7 Sample aged at 475 °C for 500 h

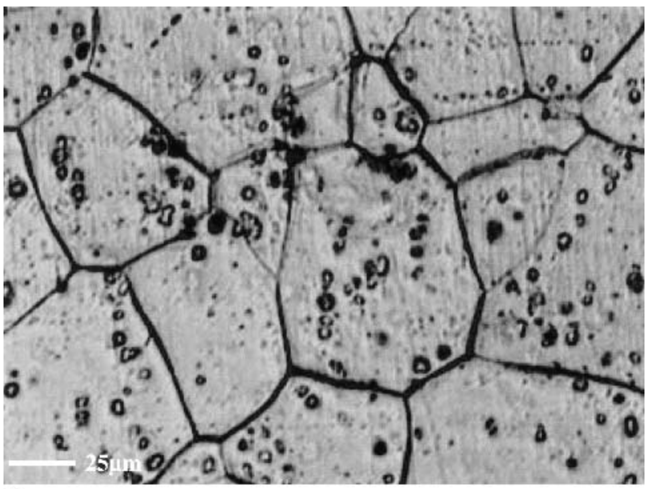

(a)

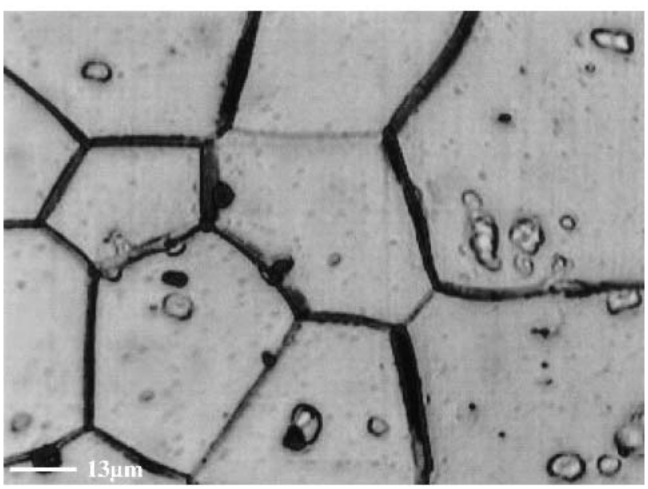

(b)

Fig. 8 Sample aged at 475 °C for 1000 h

3.2 Magnetic Properties

Figure 9 shows the behavior of coercive force with aging time. Tsuchiya et al. (Ref 5) have found an increase in the coercive force and residual induction with aging time at 475 °C in a cast duplex SS containing 12.5% ferrite. On the other hand, Maeda et al. (Ref 6) found a decrease of the coercive force with aging time at 350, 400, and 450 °C in duplex steel containing 25% ferrite. In the case of the wrought ferritic steel in this work, the coercive force did not vary with aging time either at 475 °C or 400 °C.

Previous work (Ref 7-9) has shown an increase in the T_c with aging time. Tavares and colleagues (Ref 8, 9) found an increase in T_c from 503 to 566 °C due to aging at 475 °C for 500 h in a duplex SS. Kim et al. (Ref 7) found similar results in a cast ferritic SS. In the present work, such an effect was not observed. The unaged sample and the one aged at 475 °C for 1000 h exhibited the same T_c, as is shown in Fig. 10.

The aging of high-Cr ferritic and duplex SSs promotes a broadening of the peaks in the Mössbauer spectra. A single paramagnetic peak appears at zero velocity in samples aged for long times (Ref 4). Another effect is an increase in the internal field with aging time (Ref 7). In this work, none of these effects were observed. However, the α' precipitation was detected by analysis of the hyperfine distribution curves shown in Fig. 11. The large peak at 25 T is attributed to the Fe-rich α-phase,

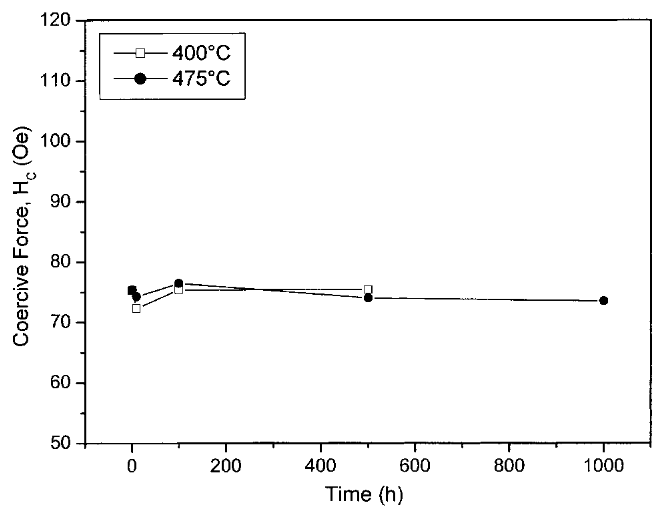

Fig. 9 Coercive force against aging time for exposure at 400 and 475 °C

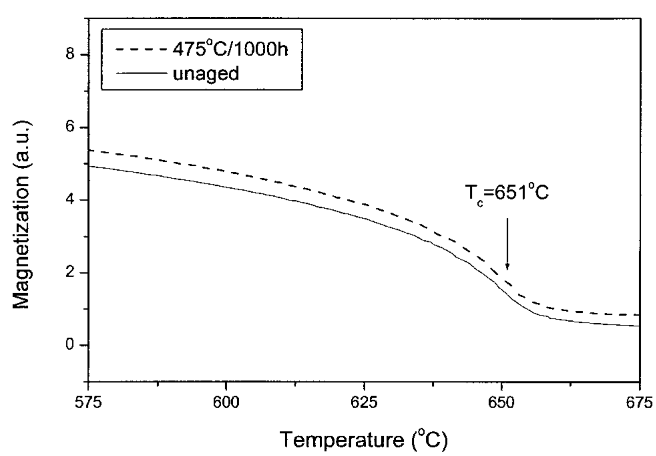

Fig. 10 Thermomagnetic analysis curves of the unaged sample and the sample aged at 475 °C for 1000 h

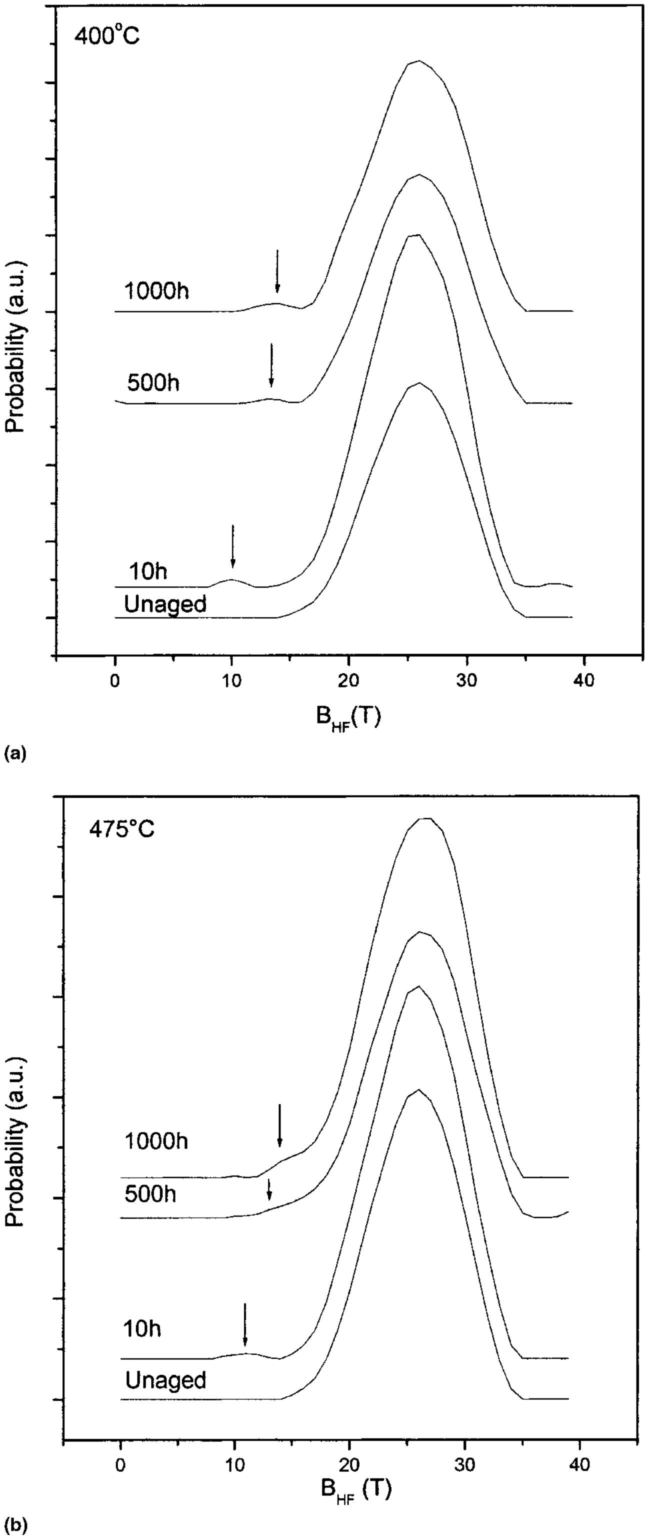

Fig. 11 Hyperfine field distribution with the aging time for exposure at (a) 400 °C and (b) 475 °C

where the ^{57}Fe atoms are surrounded by other ^{57}Fe atoms, resulting in a high hyperfine field. A small peak at about 10 to 13 T (arrows) appears in the samples aged at 400 °C (Fig. 11a) and 475 °C (Fig. 11b). This peak is attributed to the Cr-rich α′-phase, because for this phase the ^{57}Fe atom is surrounded by Cr atoms, which decrease the size of the hyperfine field (Ref 13).

Table 2 Properties obtained with the regeneration treatments compared with the aged (475 °C/1000 h) and as-received samples

Sample/condition	Hardness, HV	Toughness, J	I_r/I_a
As-received	187.0 ± 1.0	112.0 ± 1.0	0.033
475 °C/1000 h	273.5 ± 6.2	12.0 ± 1.0	0.475
475 °C + 570 °C/30 min	199.0 ± 3.5	108.0 ± 1.0	0.305
475 °C + 570 °C/1 h	190.0 ± 4.0	116.0 ± 1.0	0.015
475 °C + 675 °C/10 min	190.0 ± 5.0	118.0 ± 1.0	0.078
475 °C + 675 °C/20 min	182.0 ± 4.2	123.0 ± 1.0	0.043
475 °C + 675 °C/1 h	190.0 ± 5.1	121.0 ± 1.0	…

3.3 Regeneration of the Aged Steel

Table 2 shows the results obtained with regeneration treatments at 570 and 675 °C in samples previously aged at 475 °C for 1000 h. The heat treatments at 675 °C for 10 and 20 min promote an increase in toughness and a decrease in hardness to levels similar to those of the as-received alloy samples. The regeneration of the corrosion resistance becomes more effective with an increase in the time of the regeneration treatment from 10 to 20 min at 675 °C, and 30 min to 1 h at 570 °C. It is worth noting that an increase in time at 675 °C up to 1 h did not promote any embrittlement, which means that the formation of the σ-phase does not occur during this period at these temperatures.

4. Conclusions

The effects of aging at 400 and 475 °C on AISI 444 SS were investigated. Age-hardening curves exhibited the same general shape at both temperatures, but the hardness of the samples aged at 475 °C were higher, as expected. Overaging was not observed until 1000 h. The corrosion resistance decreased with aging time, as observed by the results of DL-EPR tests conducted at 60 °C. The ratio of I_r to I_a increased with aging time at both temperatures, but showed a particularly strong increase from 500 to 1000 h at 475 °C. The time curves for toughness versus aging exhibited similar behavior, with a pronounced decrease in toughness occurring from 500 to 1000 h at 475 °C. At the same time, metallographic observation showed an increase in intergranular attack

The effects of aging on magnetic properties were quite different from those observed in high-Cr ferritic and duplex SSs. The coercive force and the T_c did not vary with aging time. Peak broadening, paramagnetic peak appearance, and the increase of the internal field were not observed by Mössbauer spectroscopy. However, the hyperfine field distribution profile showed a small peak at low internal fields, which was attributed to the α′-phase.

Regeneration treatments at 570 and 675 °C reduced the hardness and increased the toughness of the aged samples to levels similar to that of the alloy in the unaged condition. The corrosion resistance also recovered in treatments performed at 570 °C for 1 h and at 675 °C for 20 min.

Acknowledgments

The authors are grateful to the Brazilian research agencies Fundação de Amparo à Pesquisa de Estado do Rio de Janeiro (FAPERJ); Conselho Nacional de Pesquisa (CNPq);

Agência Nacional do Petróleo (ANP); and FINEP for financial support, and to Professor Fernando Landgraf for thermomagnetic measurements and analysis.

References

1. V. Kuzucu, M. Aksoy, M.H. Korkut, and M.M. Yildirim, Effect of Niobium on the Microstructures of Ferritic Stainless Steels, *Mater. Sci. Eng., A,* Vol 230, 1997, p 75-80
2. A.C.T.M. Van Zwieten and J.H. Bulloch, Some Considerations on the Toughness Properties of Ferritic Stainless Steels: A Brief Revision, *Int. J. Press. Vessels Piping,* Vol 56, 1993, p 1-31
3. P.J. Grobner, The 885°F (475°C) Embrittlement of Ferritic Stainless Steels, *Metall. Trans.,* Vol 4, 1973, p 251-260
4. H.D. Solomon and Lionel M. Levinson, Mössbauer Effect Study of 475°C Embrittlement of Duplex and Ferritic Stainless Steels, *Acta Metall.,* Vol 28, 1978, p 429-442
5. S. Tsuchiya, Y. Ishikawa, M. Ohtaka, and T. Yoshimura, Atom Probe Study of the Aging Embrittlement of Cast Duplex Stainless Steel, *JSME Int. J. A,* Vol 38 (No. 3), 1995, p 384-392
6. N. Maeda, T. Goto, T. Kamimura, T. Naito, S. Kumano, and Y. Nakao, Changes in Electromagnetic Properties During Thermal Aging of Duplex Stainless Steel, *Int. J. Press. Vessels Piping,* Vol 71, 1997, p 7-12
7. S. Kim, W. Jae, and Y. Kim, Analysis of Phase Separation by Thermal Aging in Duplex Stainless Steels by Magnetic Methods, *J. Korean Nucl. Soc.,* Vol. 29 (No. 5), 1997, p 361-367
8. S.S.M. Tavares, M.R. da Silva, and J.M. Neto, Magnetic Properties Changes During Embrittlement of a Duplex Stainless Steel, *J. Alloys Compd.,* Vol 313, 2000, p 168-173
9. S.S.M. Tavares, R.F. de Noronha, M.R. da Silva, J.M. Neto, and S. Pairis, 475°C Embrittlement in a Duplex Stainless Steel UNS S31803, *Mater. Res.,* Vol 4 (No. 4), 2001, p 237
10. A.J. Sedricks, *Corrosion of Stainless Steel,* 2nd ed., Wiley-Interscience Publications, New York, 1996
11. N. Lopez, M. Cid, M. Puigalli, I. Azkarate, and A. Pelayo, Application of Double Loop Electrochemical Potentiodynamic Reactivation Test to Austenitic and Duplex Stainless Steels, *Mater. Sci. Eng., A*, Vol 229, 1997, p 123-128
12. C.J. Park and H.S. Kwon, Effects of Aging at 475°C on Corrosion Properties of Tungsten-Containing Duplex Stainless Steels, *Corrosion Sci.,* Vol 44, 2002, p 2817-2830
13. P.D.S. Pedrosa, "Cinética de Precipitação em um Aço Inoxidável Duplex," Master's thesis, Coordenação das Programas de Pós-Graduação em Engenharia/Universidade Federal do Rio de Janeiro (COPPE/UFRJ), Rio de Janeiro, 2001